

*Electronic Supplementary Information*

**Mammalian serum albumins as a chiral mediator library for  
bio-supramolecular photochirogenesis:  
Optimizing the enantiodifferentiating photocyclodimerization  
of 2-anthracenecarboxylate**

Masaki Nishijima,<sup>\*a</sup> Masato Goto,<sup>b</sup> Mayu Fujikawa,<sup>b</sup> Cheng, Yang,<sup>b,c</sup> Tadashi Mori,<sup>b</sup> Takehiko Wada<sup>d</sup> and Yoshihisa Inoue<sup>\*b</sup>

<sup>a</sup> Office for University-Industry Collaboration, Osaka University, 2-8 Yamada-oka, Suita 565-0871, Japan

<sup>b</sup> Department of Applied Chemistry, Osaka University, 2-1 Yamada-oka, Suita 565-0871, Japan

<sup>c</sup> Key Laboratory of Green Chemistry & Technology of Ministry of Education, College of Chemistry and State Key Laboratory of Biotherapy, West China Medical School, Sichuan University, 29 Wangjiang Road, Chengdu 610064, China

<sup>d</sup> Institute of Multidisciplinary Research for Advanced Materials, Tohoku University, Aoba-ku, Sendai 980-8577, Japan  
E-mail: nishijima@uic.osaka-u.ac.jp; inoue@chem.eng.osaka-u.ac.jp

**Table of Contents**

<b>Experimental</b>	2
<b>Table S1</b> Amino acid residues in mammalian serum albumins	3
<b>Table S2</b> Binding stoichiometries and affinities ( $K_i$ ) for the first sites of mammalian serum albumins	3
<b>Table S3</b> Enantiodifferentiating photocyclodimerization of AC mediated by SA at various AC/SA ratios	4
<b>Figure S1</b> UV and CD spectral changes upon addition of AC to a phosphate buffer solution of BSA at 25 °C	5
<b>Figure S2</b> Ellipticity changes at 330, 360, 391 and 420 nm as functions of AC/BSA ratio	5
<b>Figure S3</b> CD spectral changes upon addition of AC to a phosphate buffer solution of HSA at 25 °C and the ellipticity changes at 330, 360, 391 and 420 nm as functions of AC/HSA ratio	6
<b>Figure S4</b> CD spectral changes upon addition of AC to a phosphate buffer solution of SSA at 25 °C and the ellipticity changes at 330, 360, 391 and 420 nm as functions of AC/SSA ratio	7
<b>Figure S5</b> CD spectral changes upon addition of AC to a phosphate buffer solution of RSA at 25 °C and the ellipticity changes at 330, 360, 391 and 420 nm as functions of AC/RSA ratio	8
<b>Figure S6</b> CD spectral changes upon addition of AC to a phosphate buffer solution of PSA at 25 °C and the ellipticity changes at 330, 360, 391 and 420 nm as functions of AC/PSA ratio	9
<b>Figure S7</b> CD spectral changes upon addition of AC to a phosphate buffer solution of CSA at 25 °C and the ellipticity changes at 330, 360, 391 and 420 nm as functions of AC/CSA ratio	10
<b>Figure S8</b> Comparison of the ellipticity changes at 330, 360, 391 and 420 nm as functions of AC/SA ratio for BSA, HSA, SSA, RSA, PSA and CSA.	11
<b>Figure S9</b> Fluorescence spectral titration of AC with SSA and the determination of $K_1$ at 25 °C	12
<b>Figure S10</b> Fluorescence spectral titration of AC with RSA and the determination of $K_1$ at 25 °C	12
<b>Figure S11</b> Fluorescence spectral titration of AC with PSA and the determination of $K_1$ at 25 °C	13
<b>Figure S12</b> Fluorescence spectral titration of AC with CSA and the determination of $K_1$ at 25 °C	13
<b>Figure S13</b> Chiral HPLC traces for the AC solutions irradiated in the presence of 3 eq. CSA and 1.3 eq. PSA in phosphate buffer at 0 °C	14

## Experimental

**Materials.** Fatty acid-free bovine, human, sheep, rabbit, porcine and canine serum albumins were purchased from Sigma and used as received. 2-Anthracenecarboxylic acid (Wako), acetonitrile (Kanto), and trifluoroacetic acid (Wako) were used without further purifications.

**Instruments.** UV-vis and CD spectra were recorded on JASCO V-550 and JASCO J-720S instruments, respectively. Chiral HPLC analysis with a Hitachi L-5020 system with a L-4000 detector was run on a tandem column of Cosmosil 5C<sub>18</sub>-AR-II and Chiralcel OJ-R eluted by a 64:36 mixture of water and acetonitrile, containing 0.1% trifluoroacetic acid, at a flow rate of 0.5 mL/min.

**Spectral titration.** Serum albumin (20 mg) was dissolved in phosphate buffer at pH 7.0 (5 mL) to give a 0.06 mM solution. To the SA solution placed in a quartz cell of 5 mm light path was added stepwise a given portion of AC (5 mM) dissolved in a 10 mM NaOH solution and the resulting solution was subjected to UV-vis and CD spectral examinations. The ellipticity changes induced upon incremental addition were plotted against the AC/SA ratio to give a titration curve for each SA.

**Photoreaction and product analysis.** A fixed volume (60  $\mu$ L) of an alkaline solution of AC (5 mM) was added to phosphate buffer solutions (5 mL) at pH 7.0 containing various amounts of SA to make a series of aqueous solutions for irradiation that contained 0.6 mM AC and a varying amount of SA. Each solution (3 mL) was placed in a quartz cell, deaerated by three freeze-pump-thaw-Ar-charge cycles, and then irradiated for 1 h at  $>320$  nm under an argon atmosphere with a 300-W high-pressure mercury lamp fitted with a uranium glass filter in a thermostated water bath maintained at 0 or 25 °C. After irradiation, the conversion (the consumption of AC) was determined spectroscopically from the decrease of the AC absorbance at 390 nm, and an aliquot of the irradiated sample (0.6 mL) was diluted by the same volume of acetonitrile with stirring (to denature SA) and kept overnight in the dark. The aqueous acetonitrile solution thus obtained was ultrafiltrated with a membrane filter (Millipore; molecular cut-off 5000) and subjected to the chiral HPLC analysis under the conditions mentioned above for product distribution and enantiomeric excess.

**Table S1.** Amino acid residues in mammalian serum albumins

Amino acid	Serum albumin					
	Human <sup>a</sup>	Bovine <sup>a</sup>	Sheep <sup>b</sup>	Rabbit <sup>c</sup>	Porcine <sup>d</sup>	Canine <sup>e</sup>
Aspartic acid	36	40	44	43	37	38
Asparagine	17	14	14	12	13	14
Threonine	28	34	31	27	26	26
Serine	24	28	25	26	23	28
Glutamic acid	62	59	56	56	61	60
Glutamine	20	20	19	14	20	21
Proline	24	28	28	29	29	28
Glycine	12	16	17	20	16	22
Alanine	62	46	50	54	50	58
Valine	41	36	36	38	34	39
Cystine/2	35	35	35	35	35	35
Methionine	6	4	4	1	0	4
Isoleucine	8	14	13	16	23	54
Leucine	61	61	61	62	62	63
Tyrosine	18	20	20	24	22	21
Phenylalanine	31	27	28	24	29	30
Lysine	59	59	59	57	57	56
Histidine	16	17	19	23	18	12
Tryptophan	1	2	2	1	2	1
Arginine	24	23	22	22	26	24
<i>Difference from HSA</i>	0	66	66	89	72	57
<i>Total residues</i>	585	583	583	584	583	584
<i>Molecular mass<sup>f</sup></i>	66605	66443	66385	66148	66770	65667

<sup>a</sup> T. Peters, Jr., *All about Albumin: Biochemistry, Genetics, and Medical Applications*; Academic Press, San Diego, CA, 1996; <sup>b</sup> W. M. Brown, K. M. Dziegielewska, R. C. Foreman and N. R. Saunders, *Nucleic Acid Res.*, 1989, **17**, 10495; <sup>c</sup> S. Syed, P. D. Schuyler, M. Kulczycky and W. P. Sheffield, *Blood* 1997, **89**, 3243; <sup>d</sup> C. Hilger, M. Kohnen, F. Grigioni, C. Lehnert and F. Hentges, *Allergy* 1997, **52**, 179; <sup>e</sup> B. Pandjaitan, I. Swoboda, F. Brandejsky-Pichler, H. Rumpold, R. Valenta and S. Spitzauer, *J. Allergy Clin. Immunol.*, 2000, **105**, 279; <sup>f</sup> J. A. Loo, C. G. Edmonds and R. D. Smith, *Anal. Chem.*, 1991, **63**, 2488.

**Table S2.** Binding stoichiometries and/or affinities for the first site ( $K_1$ ) of mammalian serum albumins

SA	Number of AC bound to each site			
	1st ( $K_1/M^{-1}$ )	2nd	3rd	4th
Bovine	1 ( $5.3 \times 10^7$ ) <sup>a</sup>	3	2	3
Human	1 ( $3.0 \times 10^8$ ) <sup>b</sup>	1	3	5
Sheep	1 ( $3.8 \times 10^6$ )	4		
Rabbit	1 ( $3.4 \times 10^7$ )	3	5	~5
Porcine	1 ( $8.7 \times 10^6$ )	2	~4	
Canine	1 ( $1.2 \times 10^6$ )	2		

<sup>a</sup> T. Wada, M. Nishijima, T. Fujisawa, N. Sugahara, T. Mori, A. Nakamura and Y. Inoue, *J. Am. Chem. Soc.*, 2003, **125**, 7492; <sup>b</sup> M. Nishijima, T. Wada, T. Mori, T. C. S. Pace, C. Bohne and Y. Inoue, *J. Am. Chem. Soc.*, 2007, **129**, 3478.

**Table S3.** Enantiodifferentiating photocyclodimerization of AC mediated by SA at various AC/SA ratios<sup>a</sup>

SA	AC/SA	Temp. /°C	Conv. <sup>b</sup> /%	Yield <sup>c</sup> / % ( <i>ee</i> <sup>d</sup> /%)				<i>syn/anti</i>		HT/HH
				1	2	3	4	2/1	4/3	
None		25	80	43	36 (0)	14 (0)	7	0.8	0.5	3.8
Bovine	1.3	25	5	14	21 (-25)	32 (44)	33	1.5	1.0	0.5
		0	2	21	23 (-10)	30 (43)	26	1.1	0.9	0.8
Human <sup>e</sup>	3	25	20	42	41 (79)	11 (88)	6	1.0	0.5	4.9
		5	13	42	45 (82)	8 (90)	5	1.1	0.6	6.7
Sheep	1.3	25	19	27	21 (-18)	26 (47)	26	0.8	1.0	0.9
		0	14	32	19 (-11)	29 (51)	20	0.6	0.7	1.0
	5	25	60	34	19 (-14)	25 (44)	22	0.6	0.9	1.1
Rabbit	10	25	74	35	20 (-11)	25 (42)	20	0.6	0.8	1.2
		0	14	50	20 (54)	17 (24)	13	0.4	0.8	2.3
	5	25	41	54	19 (37)	16 (3)	11	0.4	0.7	2.7
Porcine	10	25	66	44	23 (24)	20 (4)	13	0.5	0.7	2.0
		0	4	16	69 (-89)	10 (25)	5	4.3	0.5	5.7
	5	25	34	20	33 (-64)	24 (-16)	23	1.7	1.0	1.1
	10	25	57	22	32 (-54)	25 (-28)	21	1.5	0.8	1.2
Canine	3	25	31	23	71 (94)	3 (27)	3	3.1	1.0	16
		0	42	19	77 (97)	2 (18)	2	4.1	1.0	24
	5 <sup>f</sup>	25	50	25	65 (89)	5 (12)	5	2.6	1.0	9.0
10 <sup>f</sup>	25	37	23	60 (85)	8 (8)	9	2.6	1.1	4.9	

<sup>a</sup> Irradiated at  $\lambda > 320$  nm for 1 h under Ar atmosphere (after three freeze-pump-thaw cycles) in aqueous phosphate buffer at pH 7.0; [AC] = 0.6 mM (fixed). <sup>b</sup> Consumed AC; error  $< \pm 3\%$ . <sup>c</sup> Relative yield; error  $< \pm 1\%$ . <sup>d</sup> Enantiomeric excess; error  $< \pm 3\%$ ; the positive/negative *ee* indicates predominant formation of (*M*)/(*P*)-enantiomer, respectively; see: A. Wakai, H. Fukasawa, C. Yang, T. Mori and Y. Inoue, *J. Am. Chem. Soc.*, 2012, **134**, 4990 & 10306 (erratum); Y. Kawanami, H. Tanaka, J. Mizoguchi, N. Kanehisa, G. Fukuhara, M. Nishijima, T. Mori and Y. Inoue, *Acta Cryst.*, 2013, **C69**, 1411. <sup>e</sup> M. Nishijima, T. Wada, T. Mori, T. C. S. Pace, C. Bohne and Y. Inoue, *J. Am. Chem. Soc.*, 2007, **129**, 3478. <sup>f</sup> At AC/CSA  $\geq 5$ , AC was not fully solubilized by CSA and hence the conversion could be less reliable.

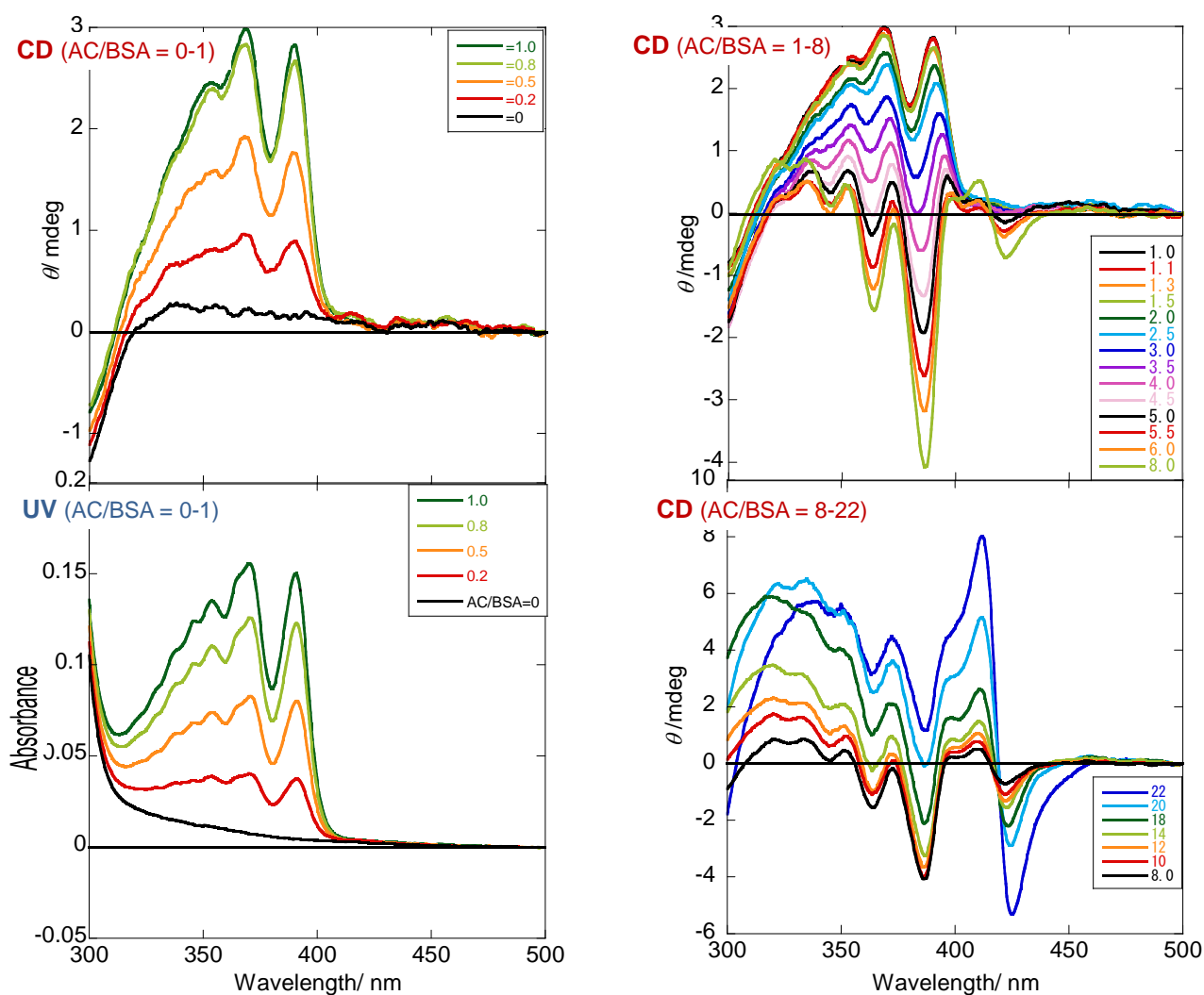


**Figure S1.** UV (bottom left) and CD spectral changes upon addition of 0-1 (top left), 1-8 (top right) and 8-22 equivalents (bottom right) of AC to a phosphate buffer solution (pH 7) of BSA (0.06 mM) at 25 °C; note that the extra couplet-like CD signals at  $\lambda > 400$  nm that rapidly grew at AC/BSA  $> 5$  (more evidently at  $> 8$ ) are likely to be artifacts arising from the yellow particles of AC formed in the solution.

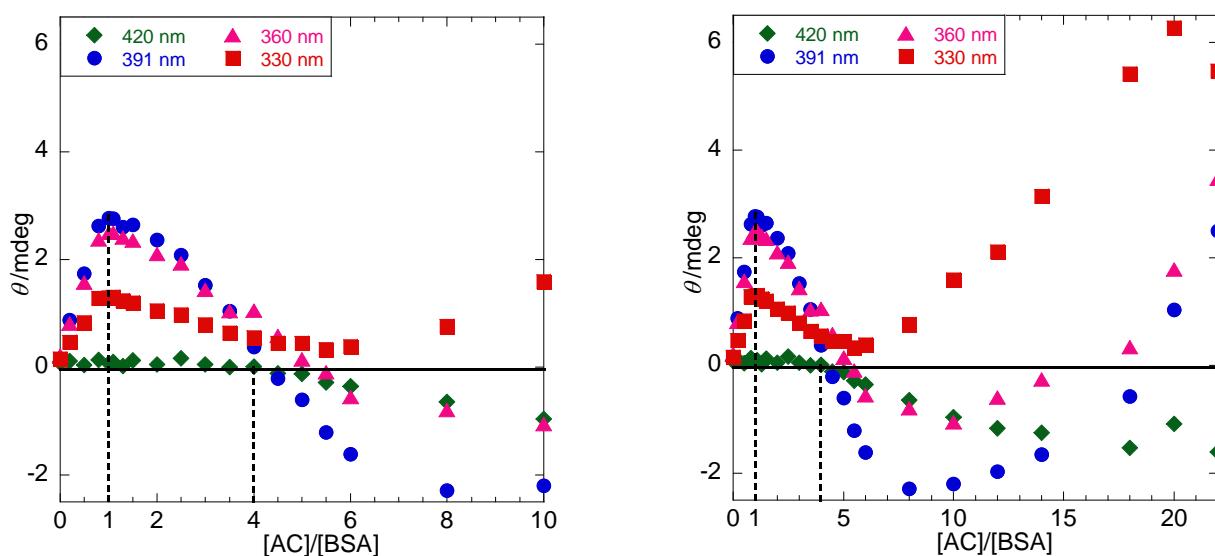


**Figure S2.** Ellipticity changes at 330, 360, 391 and 420 nm as functions of AC/BSA ratio; AC/BSA = 0-8 (left) and 0-22 (right); see Figure S1 for the original CD spectra.

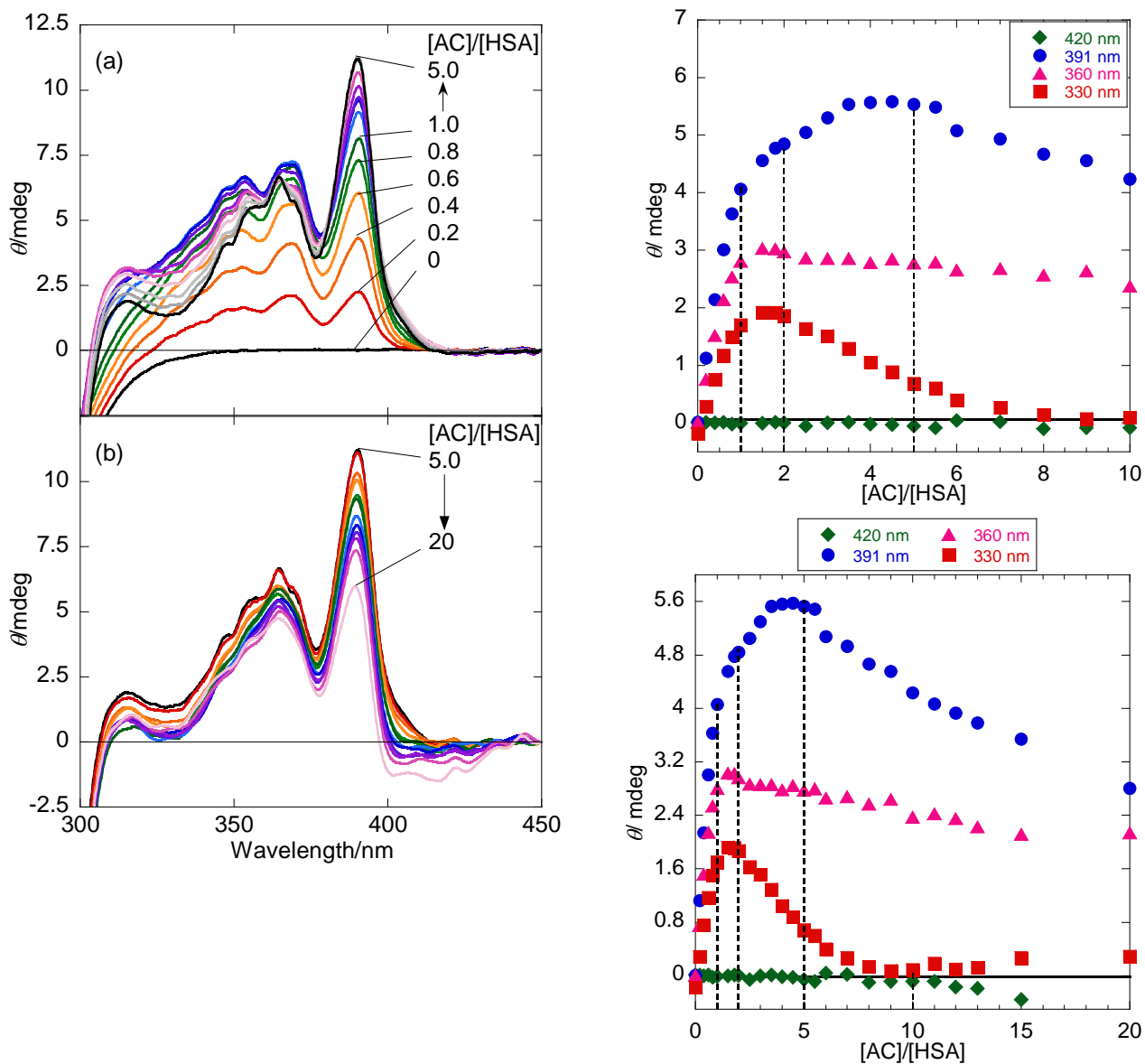


**Figure S3.** CD spectral changes upon addition of 0-5 (top left) and 5-20 equivalents (bottom left) of AC to a phosphate buffer solution (pH 7) of **HSA** (0.06 mM) at 25 °C, and the ellipticity changes at 330, 360, 391 and 420 nm as functions of AC/HSA ratio; AC/HSA = 0-10 (top right) and 0-20 (bottom right).

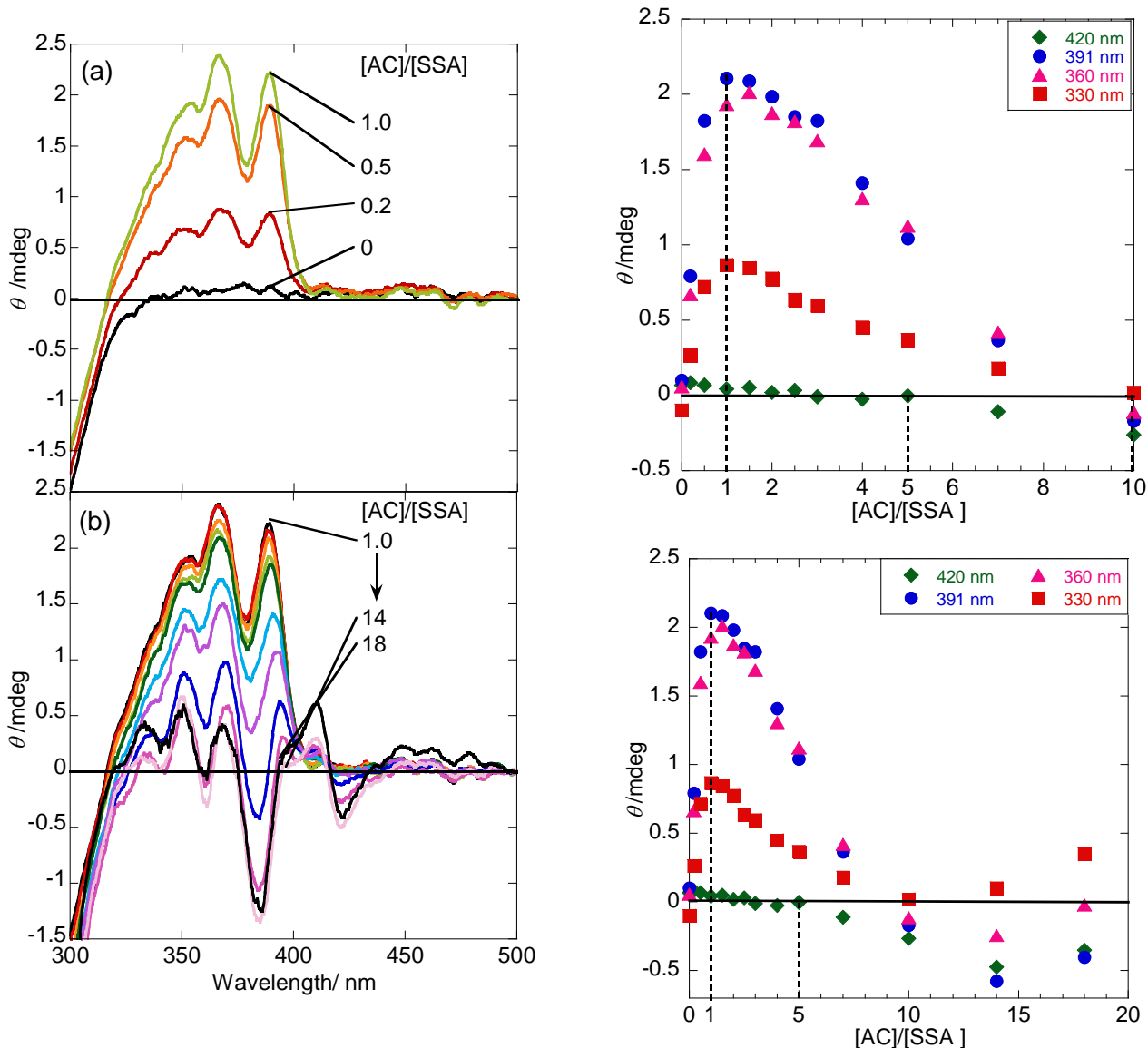


**Figure S4.** CD spectral changes upon addition of 0-1 (top left) and 1-18 equivalents (bottom left) of AC to a phosphate buffer solution (pH 7) of SSA (0.06 mM) at 25 °C, and the ellipticity changes at 330, 360, 391 and 420 nm as functions of AC/SSA ratio; AC/SSA = 0-10 (top right) and 0-20 (bottom right); note that the extra couplet-like CD signals at  $\lambda > 400$  nm that grew at AC/SSA  $> 5$  are likely to be artifacts arising from the yellow particles of AC formed in the solution.

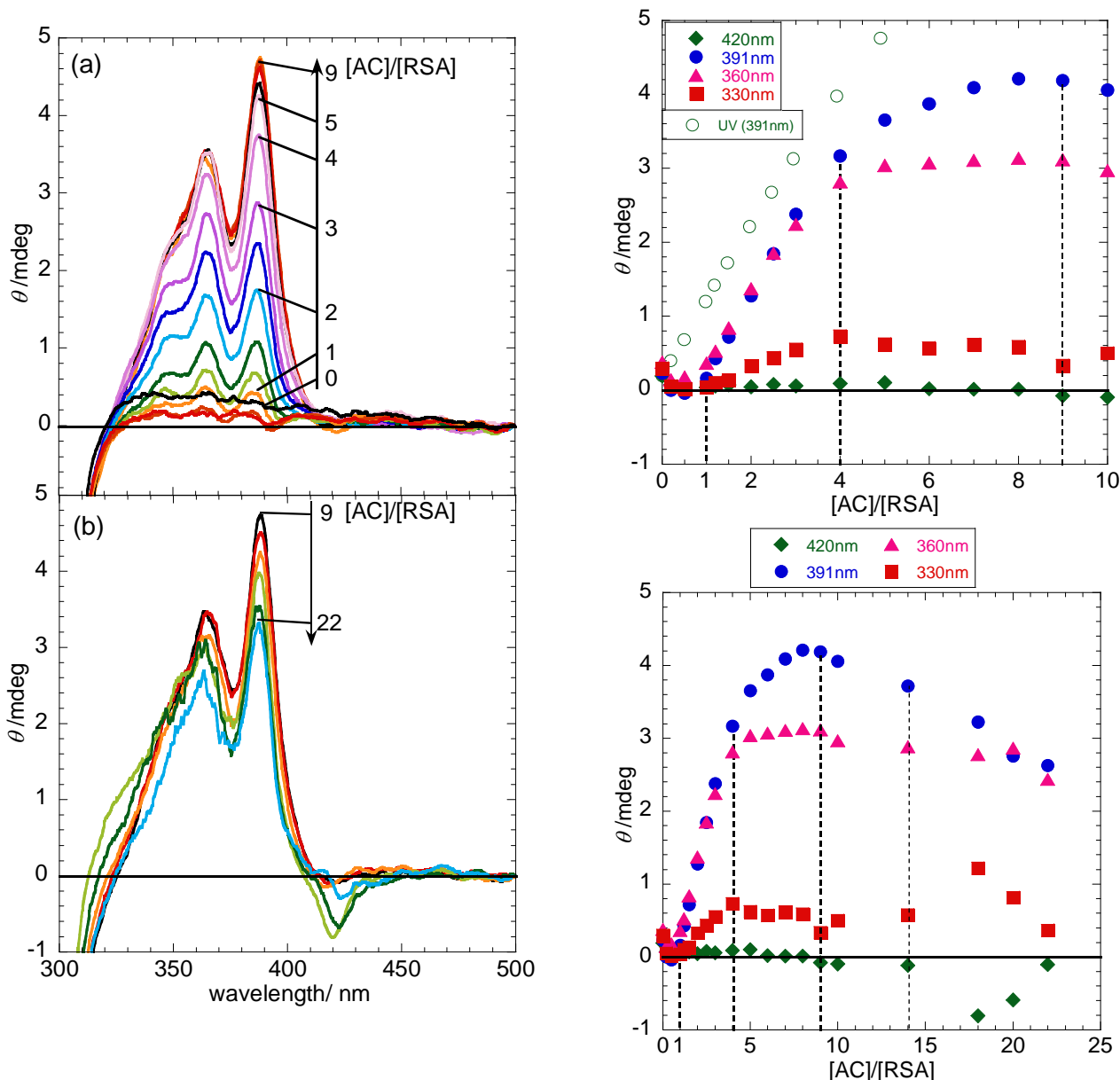


**Figure S5.** CD spectral changes upon addition of 0-9 (top left) and 9-22 equivalents (bottom left) of AC to a phosphate buffer solution (pH 7) of **RSA** (0.06 mM) at 25 °C, and the ellipticity changes at 330, 360, 391 and 420 nm as functions of AC/RSA ratio; AC/RSA = 0-10 (top right) and 0-20 (bottom right); note that the extra CD signals at  $\lambda > 400$  nm that grew at AC/RSA  $> 14$  are likely to be artifacts arising from the yellow particles of AC formed in the solution.



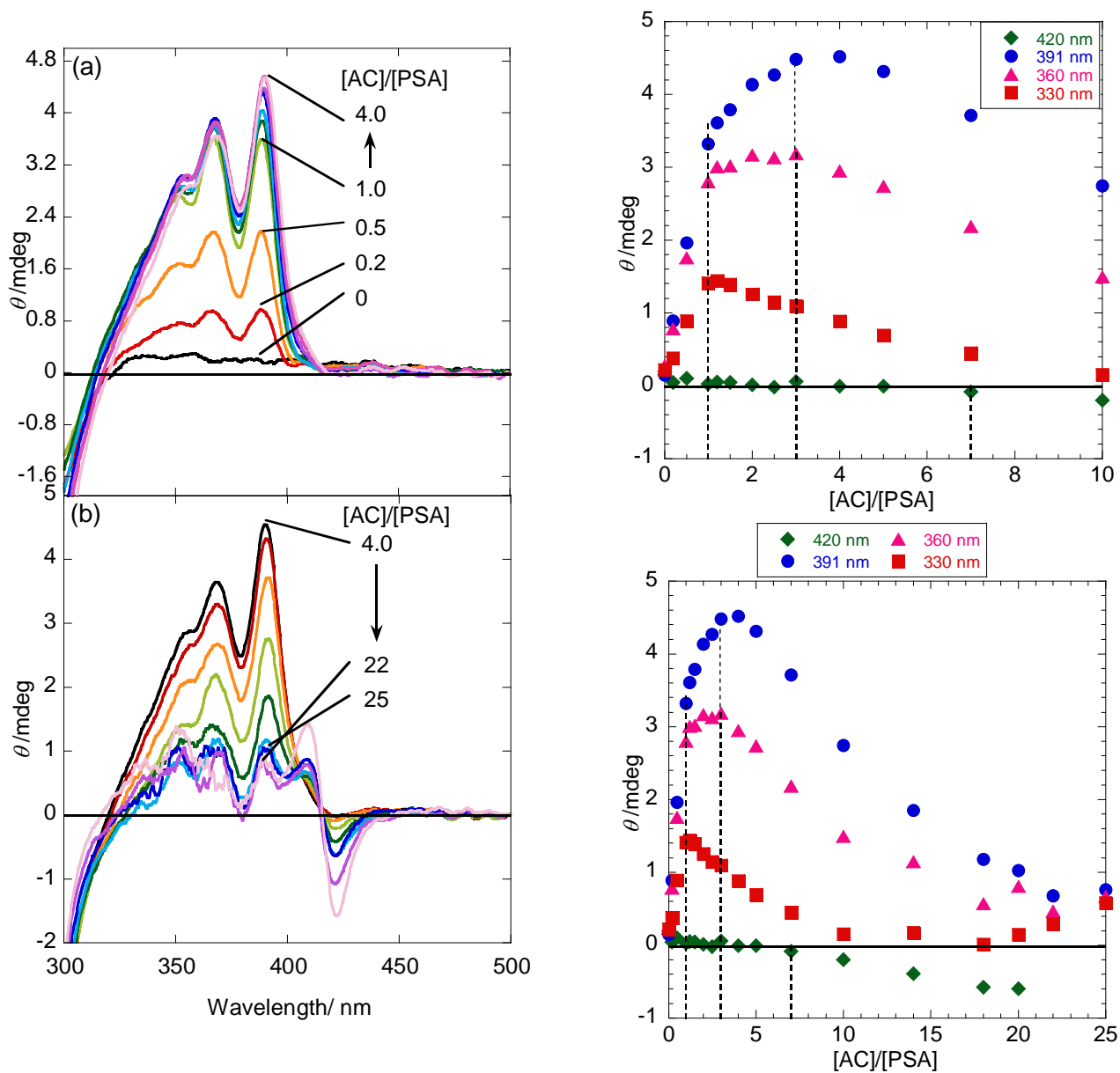


**Figure S6.** CD spectral changes upon addition of 0-4 (top left) and 4-25 equivalents (bottom left) of AC to a phosphate buffer solution (pH 7) of PSA (0.06 mM) at 25 °C, and the ellipticity changes at 330, 360, 391 and 420 nm as functions of AC/PSA ratio; AC/PSA = 0-10 (top right) and 0-20 (bottom right); note that the extra couplet-like CD signals at  $\lambda > 400$  nm that grew at AC/PSA  $> 7$  are likely to be artifacts arising from the yellow particles of AC formed in the solution.

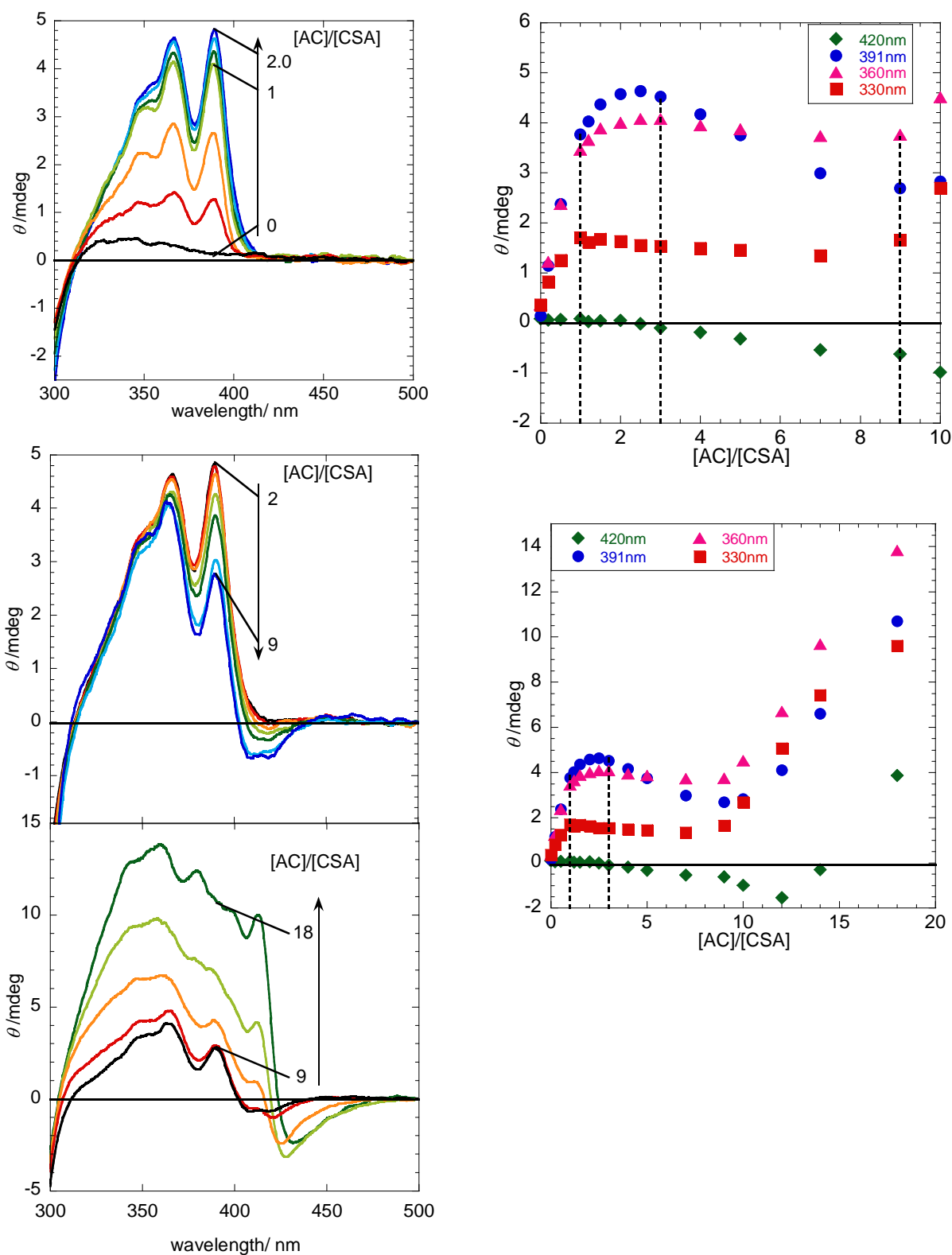


**Figure S7.** CD spectral changes upon addition of 0-2 (top left), 2-9 (middle left) and 9-18 equivalents (bottom left) of AC to a phosphate buffer solution (pH 7) of CSA (0.06 mM) at 25 °C, and the ellipticity changes at 330, 360, 391 and 420 nm as functions of AC/CSA ratio; AC/CSA = 0-10 (top right) and 0-20 (bottom right); note that the extra couplet-like CD signals at  $\lambda > 400$  nm that grew at AC/CSA  $> 3$  are likely to be artifacts arising from the yellow particles of AC formed in the solution.

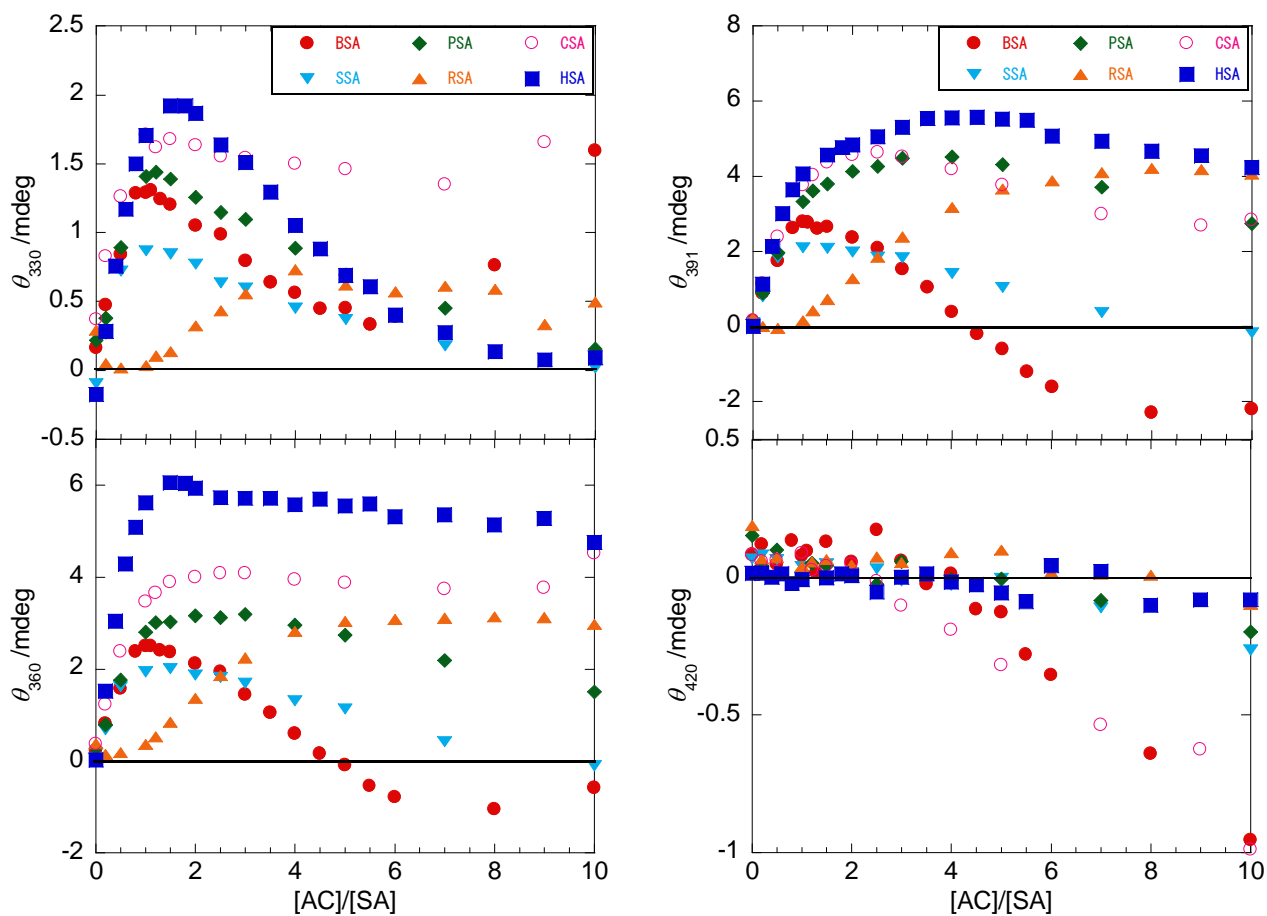


**Figure S8.** Comparison of the ellipticity changes at 330 nm (top left), 360 nm (bottom left), 391 nm (top right) and 420 nm (bottom right) as functions of AC/CSA ratio for BSA, HSA, SSA, RSA, PSA and CSA.

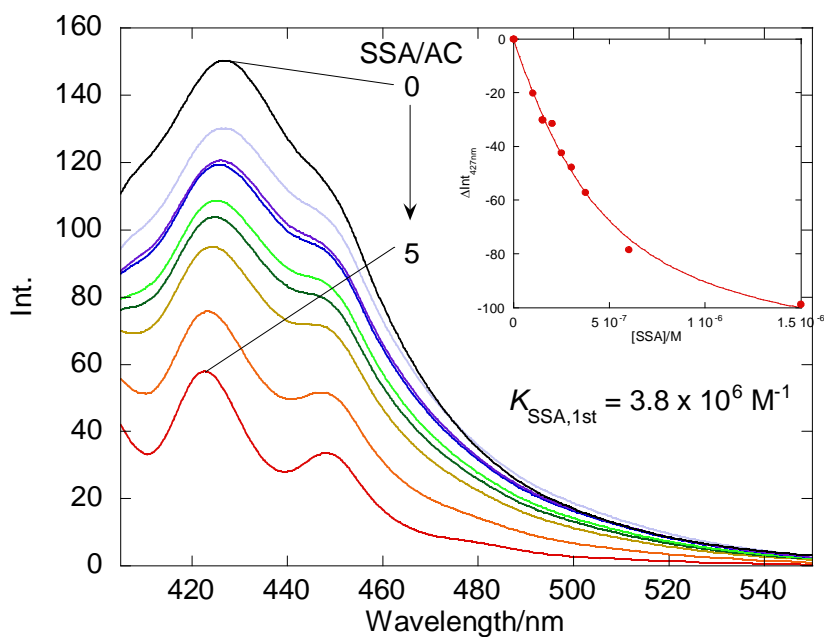


**Figure S9.** Fluorescence spectral titration of AC (0.03 mM) with SSA (0-0.15 mM) in a phosphate buffer (pH 7) at 25 °C; excitation wavelength: 390 nm. *Inset:* nonlinear least squares fit of the decrease in fluorescence intensity at 427 nm to determine the affinity of AC to the first binding site of SSA:  $K_1 = 3.8 \times 10^6 \text{ M}^{-1}$ .

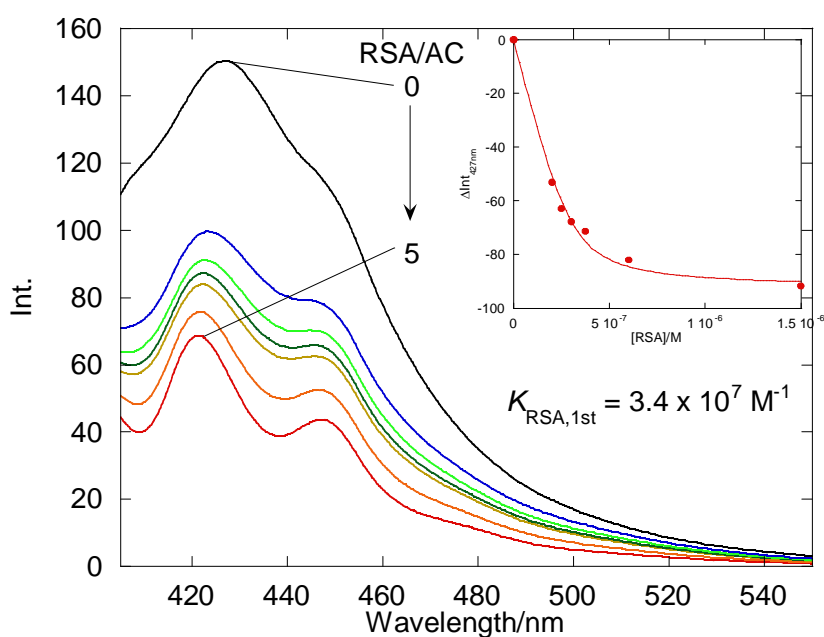


**Figure S10.** Fluorescence spectral titration of AC (0.03 mM) with RSA (0-0.15 mM) in a phosphate buffer (pH 7) at 25 °C; excitation wavelength: 390 nm. *Inset:* nonlinear least squares fit of the decrease in fluorescence intensity at 427 nm to determine the affinity of AC to the first binding site of RSA:  $K_1 = 3.4 \times 10^7 \text{ M}^{-1}$ .

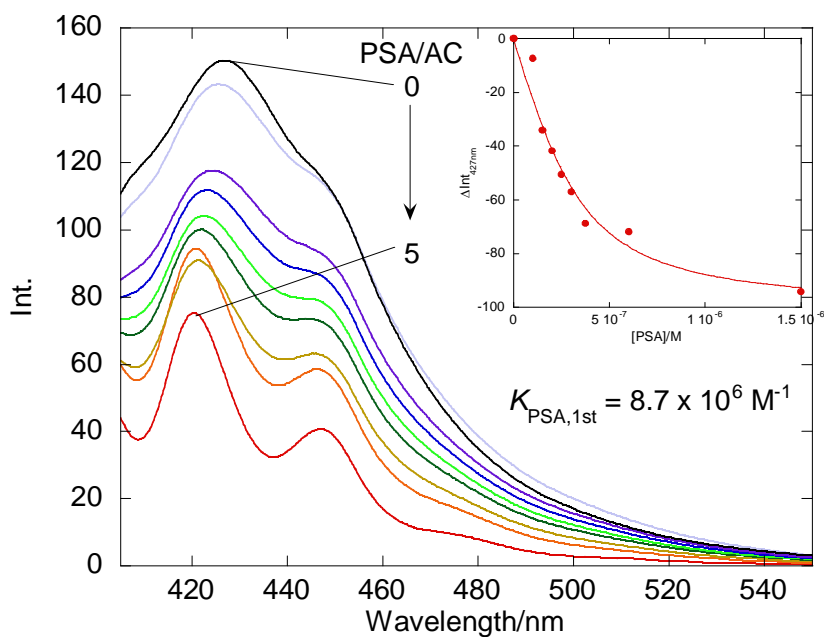


**Figure S11.** Fluorescence spectral titration of AC (0.03 mM) with PSA (0-0.15 mM) in a phosphate buffer (pH 7) at 25 °C; excitation wavelength: 390 nm. *Inset:* nonlinear least squares fit of the decrease in fluorescence intensity at 427 nm to determine the affinity of AC to the first binding site of PSA:  $K_1 = 8.7 \times 10^6 \text{ M}^{-1}$ .

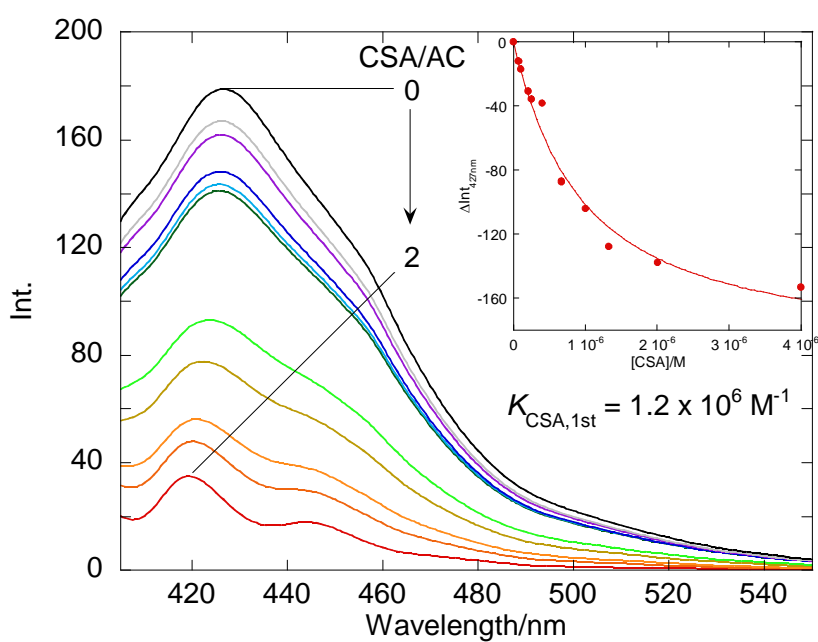


**Figure S12.** Fluorescence spectral titration of AC (0.02 mM) with CSA (0-0.04 mM) in a phosphate buffer (pH 7) at 25 °C; excitation wavelength: 380 nm. *Inset:* nonlinear least squares fit of the decrease in fluorescence intensity at 427 nm to determine the affinity of AC to the first binding site of SSA:  $K_1 = 1.2 \times 10^6 \text{ M}^{-1}$ .

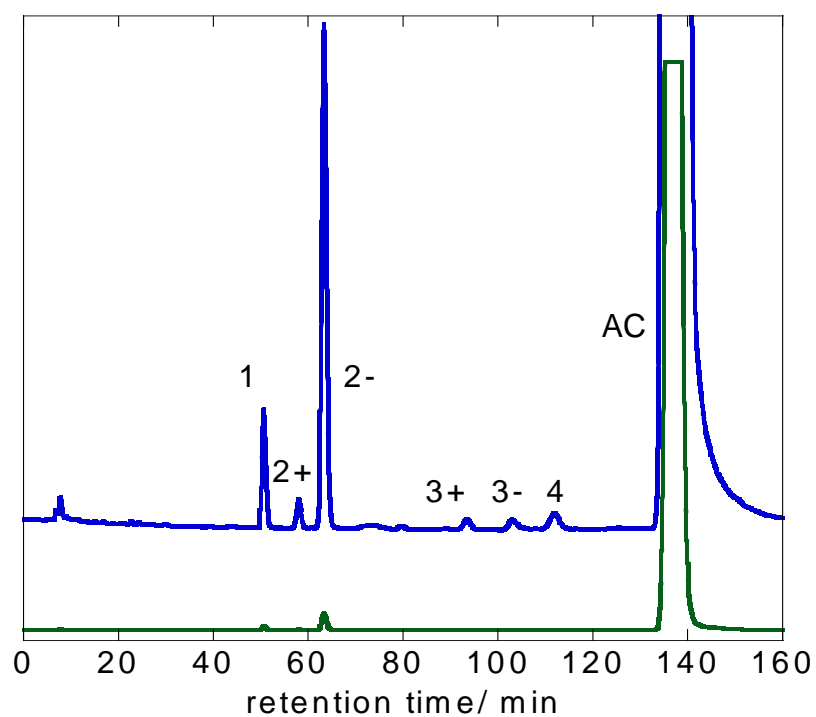
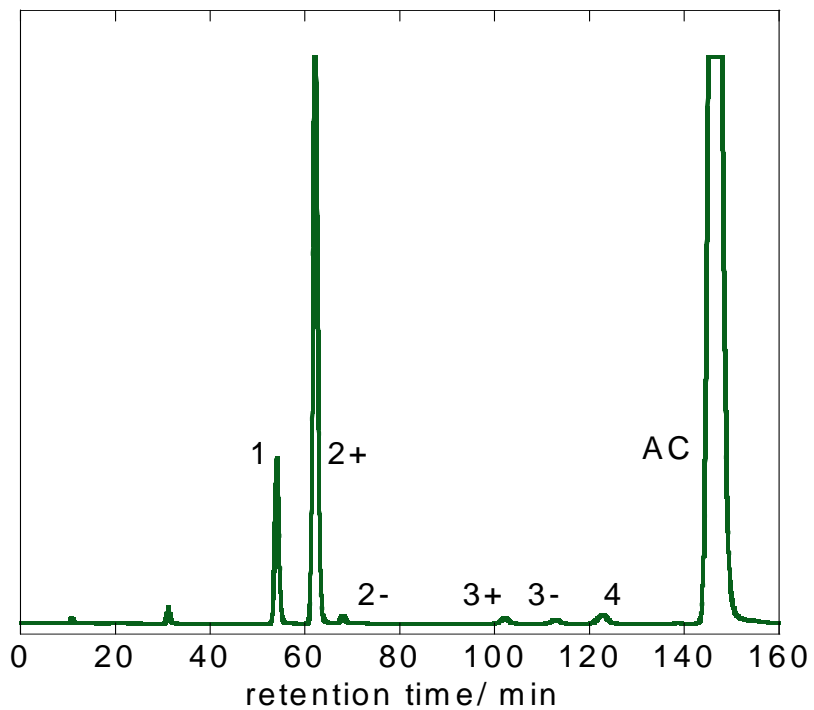


**Figure S13.** Chiral HPLC traces for the AC solutions irradiated in the presence of 3 eq. CSA (top) and 1.3 eq. PSA (bottom) in phosphate buffer (pH 7) at 0 °C.